CMS Physics Analysis Summary

Contact: cms-pag-conveners-exotica@cern.ch 2009/07/16

Searching for Majorana Neutrinos in the Like-Sign Dilepton Final State at $\sqrt{s} = 10$ TeV at the LHC

The CMS Collaboration

Abstract

The Standard Model can be extended to include massive neutrinos as observed in the recent oscillation experiments. Perhaps the most commonly studied model is the type-I seesaw mechanism. This model introduces a new neutrino with a Majorana nature and an unknown mass. In this study we conclude that the CMS detector has the potential to reach a discovery in a first year at 10 TeV startup collision energy, for a nominal integrated of 100 pb^{-1}, in a Majorana neutrino mass range near 100 GeV.

1 Introduction

The non-zero masses of the neutrinos that have been recently confirmed from the oscillation experiments [1] is arguably the first evidence for physics beyond the SM. The tiny values of the observed neutrino mass aggravate the lack of our understanding of mass generation for elementary particles. The leading theoretical candidate to explain neutrino masses is the so-called "see-saw" mechanism: The smallness of the observed neutrino masses is due to the largeness of a mass of a new heavy state N, $m_\nu \sim y_\nu^2 v^2 / M_N$, where y_ν is a Yukawa coupling and v is the Higgs vacuum expectation value in the Standard Model. Due to the new heavy neutrino's Majorana nature, it is its own anti-particle which allows for decays which violates the lepton number conservation by two units. Searching for the Majorana neutrinos in experiments is thus of fundamental importance.

Since the LHC is going to take us to a new energy frontier, it is appealing to consider the search for the heavy Majorana neutrinos in the LHC experiments. In this note, we perform a detailed simulation and assess the signal observability at the LHC with the CMS detector. Since the initial start-up center-of-mass energy for the LHC collisions is expected to be 10 TeV, and a Majorana Neutrino could be an early physics discovery at the LHC, this study has been done using 10 TeV Monte Carlo processed with the CMS detector simulation.

2 Monte Carlo Generation and Detector Simulation of Majorana Neutrino and Background Events

2.1 Majorana Neutrino

The Majorana nature of the neutrino allows for lepton number violation via dilepton production without any $E_{\mathrm{T}}^{\mathrm{miss}}$. Production of a Majorana neutrino at a hadron collider can occur via two processes: vector boson fusion (Fig. 1) or virtual W decay (Fig. 2), both of which result in lepton number violation. Since vector boson fusion is significantly suppressed by the matrix element $|V_{N\ell}|^4$ [2], we focused only on the resonance production in this study; furthermore, we search for a Majorana neutrino in the like-sign di-muon final state with jets.

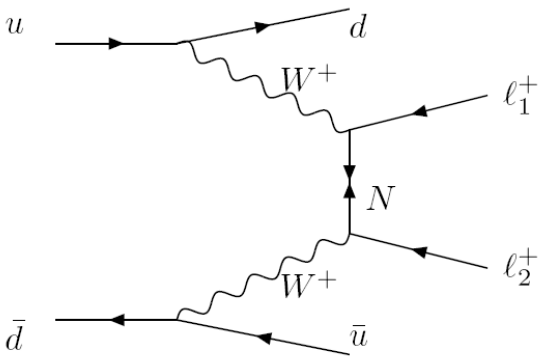

Figure 1: The Feynman diagram for a Majorana neutrino (N) produced via vector boson fusion. The cross section for this process is suppressed by $|\ V_{N\ell}\ |^4$.

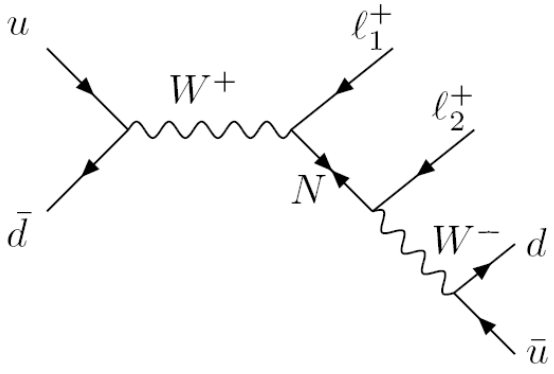

Figure 2: The Feynman diagram for resonance production of a Majorana neutrino (N). This production method is explored in this study.

Table 1: The expected event rate for Majorana neutrinos at $s = \sqrt{10}$ TeV collisions at the LHC for a nominal integrated luminosity of 100 pb^{-1}.

M_N	Cross-section (pb)	Event Rate (100 pb^{-1})	Number MC Events
100 GeV	3.17	317	50k
120 GeV	1.24	124	5k
140 GeV	0.632	63.2	5k
160 GeV	0.362	36.2	5k
180 GeV	0.227	22.7	5k
200 GeV	0.152	15.2	50k

Table 2: Standard Model backgrounds used in the analysis.

Background	Cross-Section (pb)	Event Rate (100 pb^{-1})	Number MC Events
WW	74	7400	200k
ZZ	10.5	1050	200k
tW	32	3200	170k
WZ	32	3200	250k
Triple W/Z	0.071	7.1	200k
Drell-Yan $M_{\mu\mu} > 200$ GeV	1.5	150	10k
$Z(\mu\mu)$ + jets	657	65700	900k
$Z(\tau\tau)$	1086	108600	1.2M
VQQ (V=W/Z Q=b/c)	289	28900	1M
$t\bar{t}$	414	41400	2M

There are two reasons that we used like-sign muon signature: there is a rather restrictive bound on electron Majorana neutrino coupling from the non-observation of neutrino-less double β decay [2], and the CMS detector has an excellent muon detection system with very low charge misidentification. This note covers the potential of early discovery region between the large Majorana neutrino masses 100 GeV and 200 GeV. This model has not yet been studied so there are no experimental limits set by the Tevatron or other experiment. Therefore, we have studied a mass range beginning near the Z boson mass.

An initial weighted matrix-element calculation was done for the production of Majorana neutrinos via proton-proton collisions at 10 TeV with the final products as shown in Fig. 2. The resulting output was in the Les Houches 1.0 format [3]. These data sets were then unweighted using PYTHIA [4] version 6.4 to generate events for each neutrino mass. The generated events files were interfaced with CMS Software, CMSSW, version 2_1_17 where parton showering, vertex smearing, GEANT4 [5] detector simulation, digitization of simulated electronics signal, and reconstruction were performed. The details of the data sets are summarized in Table 1.

2.2 Backgrounds

There are various Standard Model backgrounds that must be considered. Most processes that have two isolated muons contribute to the background. The individual contributions from the background events are much smaller than the number of expected signal events, so there is a good chance for an early discovery of a Majorana neutrino in the mass range studied here.

The Standard Model backgrounds included in this study are listed in Table 2. Most of the background samples were produced as part of the official production run for Monte Carlo physics studies being prepared in anticipation of the LHC start-up. There were no official Drell-Yan data sets with an invariant $M_{\mu\mu}$ below 200 GeV; however the Z($\mu\mu$) data set is available in $\hat{p}_T$ bins starting from zero so we have coverage over a similar phase space. The triple-gauge-boson data samples ($W^{\pm}W^{\pm}W^{\mp}$, $W^{\pm}W^{\pm}Z$, $W^{\pm}ZZ$, ZZZ) were produced privately. We first generated them using COMPHEP 41.10 [6] and then processed them with CMSSW 2_1_17 in the same manner as the signal data sets.

3 Event Selection

As mentioned, the signal signature is characterized by two like-sign muons. In addition to these muons, the Majorana Neutrino also produces an accompanying W boson during its decay. We look for signatures in which the W decays to two jets, as this allows us to consider final states without light neutrinos. While there is no true $E_{\mathrm{T}}^{\mathrm{miss}}$ in the signal, we do not rely on this fact for the event selection because the $E_{\mathrm{T}}^{\mathrm{miss}}$ resolution and tails during the LHC's initial start-up may not be well characterized.

3.1 Trigger

A detailed description of the CMS Level-1 (L1) and High Level (HLT) triggers can be found in Ref. [7]. There are two main L1 muon trigger paths, a single muon trigger with a nominal p_{T} threshold of 7 GeV and a di-muon trigger with a nominal p_{T} threshold of 3 GeV. As we are interested in the di-muon signatures we plan to use the HLTDoubleMu3 HLT trigger, which is based upon the L1DoubleMu3, and is available in both of the initial start-up trigger menus, 8E29 and 1E31. The Majorana neutrino events passing our selection cuts have trigger efficiency of 88.8% and 88.1% for the 100 GeV M_N and the 200 GeV M_N, respectively. We can increase our trigger efficiency by including the single muon HLT. There are two that may be used with from the 1E31 start up trigger tables. The HLTMu9 and HLTMu11 triggers required a single muon L1 trigger with 9 and 11 GeV respectively. If we include these triggers the trigger efficiency on events passing the selection cuts is 97.5% and 97.7% for the 100 GeV and the 200 GeV M_N data sets respectively.

3.2 Muon Selection

For those events that pass the trigger we impose several additional cuts. We start by looking for global muons that pass quality cuts. The number of reconstructed hits belonging to the muon's track in the silicon tracker is required to be greater than 10 and the global muon fit's χ^2 must be less than 10 per degree of freedom.

If the event has at least two global muons that pass the quality cuts we then require that both leading muons have $p_{\mathrm{T}} > 15$ GeV. The muon p_{T} distributions for both signal masses are shown in Fig. 3. For the lower mass range the muon p_{T} for both muon's is low due to the Majorana neutrino's mass being close to the mass of the W boson. For the higher Majorana neutrino mass the p_{T} of the muons is no longer suppressed.

After the p_{T} cuts we impose isolation cuts. Presently we are using the simplest isolation requirements suggested by the muon particle object group, POG, [8]. These requirements are that the sum of the p_{T} of the tracks other than the muon's within a ΔR cone of 0.3 be less than 3 GeV and that the sum of E_T of the calorimeter deposits within the same ΔR cone be less than 5 GeV.

Table 3: Muon selection, individual cut efficiencies

		% Events Accepted			
	Total Events	2 SS Quality	2 with $p_T > 15$ GeV	2 Isolation	All
100 GeV Signal	49400	72.7%	38.2%	60.0%	30.0%
200 GeV Signal	49899	74.2%	70.9%	63.8%	60.9%
$t\bar{t}$	1933780	4.7%	2.5%	1.5%	1.2×10^{-4}
tW	169048	3.1%	2.0%	1.7%	5.3×10^{-5}
WW	203591	0.28%	0.74%	0.94%	4.9×10^{-6}
ZZ	200564	0.89%	4.0%	4.2%	2.0×10^{-4}
WZ	249100	0.81%	0.25%	2.0%	2.0%
$WZ \rightarrow$3l+jj	5000	12%	27%	27%	2.2%
DY/ZmumuJet	890324	1.8%	0.15%	1.5%	1.9×10^{-5}
Z(tautau)	1245500	0.14%	0.22%	1.0%	4.8×10^{-6}
VQQ	1006772	13.0%	74.5%	80.9%	2.2×10^{-5}
Triple W/Z	190000	2.0%	36%	44%	0.24%

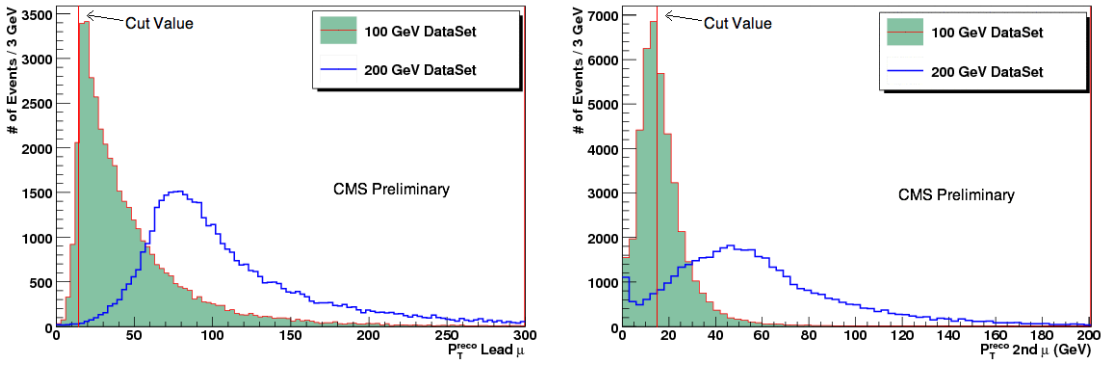

(a) (b)

Figure 3: The muon p_T distributions for both the 200 GeV (blue line) and the 100 GeV (solid green) signal data sets. The reconstructed leading muon p_T is shown in (a) and the second leading reconstructed muon's p_T is shown in (b).

We require that the event has exactly two isolated global muons passing the quality, p_T, and isolation cuts, and that they be like-sign. The charge misidentification rates for the CMS detector are expected to be very low, especially for global muons. We require that the charge from the global fit and the tracker system fit match. These cuts remove nearly all of backgrounds, while still having a reasonable acceptance for the Majorana neutrino. This is seen in Table 3 which gives the percentage values of remaining events for each cut. The columns reflect the fact that muon quality, isolation and like-sign requirements are correlated when their production comes from quark cascade decays. This is particularly evident in the VQQ data set. Thus, despite its relatively large cross-section, VQQ and $t\bar{t}$ is heavily suppressed by the muon selection requirements.

3.3 Jets

The remaining final state particles are the two jets produced from the W boson decay. We choose to search for hadronically decaying W bosons as this allows for the requirement for exactly two like-sign muons and does not lead to light neutrinos. We chose to use iterative cone jets with the cone radius of 0.5, which are created as part of standard CMS reconstruction. Further details regarding the cone jet reconstruction methods and efficiencies of the CMS detector can be found in Refs. [8, 9]. The jets are then corrected using the standard CMSSW L2+L3 jet correction packages, which correct for detector response in η and p_T [10]. Currently both of these corrections are based on Monte Carlo QCD jets. The CMS jet energy correction group plans to implement data-driven methods once data become is available [10]. Events are required to have at least two jets with corrected $p_T > 30$ GeV (Fig. 4). The jets are further combined to form the W mass. In the case where there are more than two jets meeting the p_T requirement the two that best combine to the W mass are chosen. The jet selection cut has a large acceptance on both signal and background data sets, as shown in Table 4. The primary use of the jet requirement is for Majorana neutrino mass reconstruction. Additionally it helps in the suppression of the Drell-Yan background, and the di and tri gauge boson backgrounds due correlations between the number of leptons and the number of jets in the gauge boson decays.

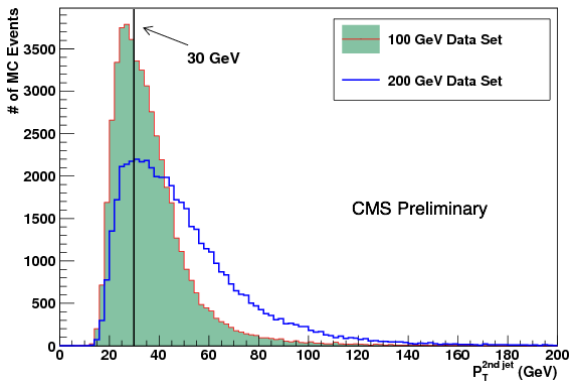

Figure 4: The p_T of the leading two jets for the two signal data sets. Events are required to have two jets above the 30 GeV cut shown.

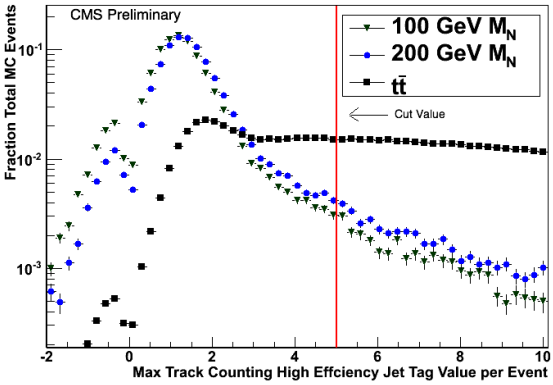

Figure 5: The largest jet tag discriminator value for each signal event is plotted for the 100 GeV and 200 GeV M_N data sets and the $t\bar{t}$ data set. The vertical line shows the cut value.

We considered one additional background not listed on Table 4, W+jets. An analysis of a Monte

Table 4: Event selection acceptance by individual selection cuts

Data Set	Total Events	Selection Cuts				Nb. of Events
		Muon	Jet	No Tagged b_{jet}	All Cuts	100 pb^{-1}
100 GeV Signal	49400	30.0%	60.0%	96.2%	14.7%	46
200 GeV Signal	49899	60.9%	78.6%	94.2%	39.2%	6.0
$t\bar{t}$	1983780	0.012%	99.1%	25.6%	3.5×10^{-5}	1.5
tW	169048	5.3×10^{-5}	96.6%	42.1%	2.4×10^{-5}	0.076
WW	203591	4.9×10^{-6}	78.7%	94.4%	$< 4.9 \times 10^{-6}$	< 0.036
ZZ	200564	0.020%	76.6%	81.2%	4.0×10^{-5}	0.042
WZ	249100	0.061%	76.9%	88.1%	8.0×10^{-5}	0.26
$WZ\rightarrow$3l+jj	5000	2.2%	90.4%	95.6	4.0×10^{-4}	0.0071
DY/ZmumuJet	890324	2.2×10^{-5}	22.2%	97.4%	3.1×10^{-6}	0.14
Z(tautau)	1245500	4.8×10^{-6}	30.6%	97.5%	$< 8.0 \times 10^{-7}$	< 0.086
VQQ	1006772	2.2×10^{-5}	26.0%	91.1%	9.9×10^{-7}	0.029
Triple W/Z	190000	0.24%	94.2%	80.9%	0.10%	0.011

Carlo data set equivalent to 250 pb^{-1} and had no events pass our selection cuts. Up to the limits of statistics this agrees with the results from the VQQ data set which included W+$c\bar{c}$ and W+$b\bar{b}$.

3.4 b-tagging

The final selection cut we use is a veto on events that contain a jet, which has been tagged as coming from a b-quark. There are several b-tagging algorithms available in CMS, which offer various purity and efficiency levels. Each of the algorithms assigns a discriminant value to the jets within a specified jet collection. The higher values are more likely to have originated from a b-quark. In our case purity is not important as the removal of b-quarks is the goal of this selection, but the efficiency is important; therefore we choose to use the track counting algorithm. This algorithm calculates a signed impact parameter for all the tracks that have been associated with each jet and orders them by decreasing significance; the b-tag discriminator is then defined as the significance of the either the second or third track [11]. The high efficiency algorithm uses the second track. Based upon the tagged values for the jets in the signal sample a discriminator value of 5 is chosen as the b-tag veto value, as shown in Fig. 5. This operating point has a light quark (d, u, and s mis-tag rate of 0.01 and a b-tagging efficiency of 0.62 [11]. This cut does not have a significant impact on the backgrounds that were studied in detail, with the exception of the top quark data sets ($t\bar{t}$ and tW). (see Table 4) The additional events that are expected to be removed by this cut from the b-quark and QCD backgrounds are also important.

4 QCD Background Estimates

The backgrounds from QCD events are difficult to estimate in a standard direct way via Monte Carlo simulation and application of selection cuts due to their large cross sections. As part of the official Monte Carlo production, large data sets of these backgrounds were produced, which enable us to consider a factorized approach. This approach is to look at the probabilities of an event to pass the selection cuts separately and then combine these efficiencies for a factorized estimation of the number of remaining events [12]. We must consider any correlation between our selection cuts (as is seen e.g. for the WZ background, see section 5), and have therefore investigated each of the cut efficiencies that may have correlation separately

Table 5: The efficiencies used in the factorization calculations.

QCD Data	Jet ϵ (Num. MC Events)			b tag veto ϵ (Num. MC Events)	
Bins (GeV)	2 Jets	1 Iso Mu + 1 Jet	1 Iso Mu + 2 Jets	only veto	with 1 Global Mu
$15 < \hat{p}_T < 30$	5.56×10^{-3}	1.03×10^{-6}(2)	-	0.994	2.06×10^{-6}(40)
$30 < \hat{p}_T < 50$	0.200	1.77×10^{-5}(33)	6.45×10^{-6}(12)	0.976	5.23×10^{-4}(973)
$50 < \hat{p}_T < 80$	0.511	7.57×10^{-5}(55)	5.10×10^{-5}(37)	0.952	1.60×10^{-3}(1165)
$80 < \hat{p}_T < 120$	0.793	2.26×10^{-4}(11)	2.26×10^{-4}(11)	0.919	4.26×10^{-3}(207)
$120 < \hat{p}_T < 170$	0.878	1.11×10^{-4}(6)	9.24×10^{-5}(5)	0.890	6.37×10^{-3}(345)
$170 < \hat{p}_T < 230$	0.935	2.06×10^{-5}(1)	2.06×10^{-5}(1)	0.865	0.0102(496)

and together. There are three resulting calculations we could use. As they give similar results, we choose to use Eq. 2, since it only contains only two efficiencies which helps to reduce the systematic uncertainty in this analysis.

$$N_{expected}(2\mu + 2jets + bjetveto) = \sigma \times \mathcal{L} \times \epsilon^2_{1Iso\mu} \times \epsilon^{p_T>30\,\mathrm{GeV}}_{2jets} \times BF_{SS\mu} \times \epsilon_{bjetveto}; \quad (1)$$

$$N_{expected}(2\mu + 2jets + bjetveto) = \sigma \times \mathcal{L} \times \epsilon^2_{1Iso\mu\&1Jet} \times BF_{SS\mu} \times \epsilon_{bjetveto}; \quad (2)$$

$$N_{expected}(2\mu + 2jets + bjetveto) = \sigma \times \mathcal{L} \times \epsilon_{1Iso\mu} \times \epsilon_{1Iso\mu\&2jets} \times BF_{SS\mu} \times \epsilon_{bjetveto}. \quad (3)$$

Here σ is the cross section of the data set, $\mathcal{L}$ is the integrated luminosity. The $BF_{SS\mu}$ is the fraction of events with two like-sign muons. The ϵ variables are the efficiencies of our selection cuts: $\epsilon_{1Iso\mu}$ is the efficiency of finding one isolated global muons, $\epsilon^{p_T>30\,\mathrm{GeV}}_{2jets}$ is the efficiency of finding 2 jets, $\epsilon_{1Iso\mu\&1Jet}$ is the efficiency of finding one global isolated muon and 1 jet, $\epsilon_{1Iso\mu\&2jets}$ is the efficiency of finding one global isolated muon and 2 jets, and $\epsilon_{bjetveto}$ is the efficiency of finding on jet tagged as a b quark. The muons are always required to have a p_T above 15 GeV and the jets are required to have a corrected p_T above 30 GeV. The efficiencies are all calculated with respect to the number of total Monte Carlo events. We do not have enough statistics to calculate the $BF_{SS\mu}$ for each of the $\hat{p}_T$ QCD bins. The average was found from the data sets which had sufficient statistics, and was used in the calculations. In the case where most of the same sign muons would come from b-quark cascade decays, we would expect the value to be close to 20%. If the muons are mostly coming from random decays, we would expect the value to be close to 50%. The average calculated using global muons and the upper 60% of the $\hat{p}_T$ range is 27.3%, if stand-alone muons are used, there is sufficient statistics across the entire $\hat{p}_T$ range and the average is 24.5%. For these calculations we used two standard CMS production QCD samples one with lower $\hat{p}_T$ limits and no upper $\hat{p}_T$ limits and one that is binned with upper $\hat{p}_T$ limits. As in the lower $\hat{p}_T$ regions there were not large statistics in the binned data sets, therefore, we used the higher statistics from the unbinned data and imposed an upper $\hat{p}_T$ cuts on the unbinned data sets to avoid double counting. The efficiencies used for all three calculations are shown in Table 5 for each $\hat{p}_T$ range. The final results for all three methods are shown in Table 6. The QCD background is the dominant Standard Model background to our study. Based upon the results of the factorized approach we expect 3 QCD events to make it through the selection cuts at 100 pb^{-1}.

Although the factorization method gives us a handle to understand the contribution from QCD background, it is not the only method that can be used. We can introduce a data driven technique for controlling the fake rate of leptons in QCD events, which is also applicable to other samples. This method is described in detail in Ref. [13] to understand the background of Higgs

Table 6: The expected number of events of the QCD backgrounds studied via a factorized extrapolation of the cut efficiencies.

QCD Data Set	Nb. of Events (100 pb^{-1})			
$\hat{p}_T$ Bins (GeV)	Method 1	Method 2	Method 3	Standard Analysis Result
$15 < \hat{p}_T < 30$	0.026	0.038	< 0.022	0
$30 < \hat{p}_T < 50$	1.0	0.78	0.73	0
$50 < \hat{p}_T < 80$	2.0	1.8	1.8	0
$80 < \hat{p}_T < 120$	0.19	0.21	0.21	0
$120 < \hat{p}_T < 170$	0.066	0.076	0.063	0
$170 < \hat{p}_T < 230$	4.5×10^{-4}	4.8×10^{-4}	4.8×10^{-4}	0
QCD Total	3.3	2.9	< 2.8	0

particle production where it decays into W bosons. The method discussed in this study involves leptonically decaying W bosons, therefore a similar method can also be used for our analysis. The fake rate is obtained by using the probability of a muon being faked. This probability is found by observing the number of muons that match to one of a collection of candidates which are considered muon faking candidates. The most appropriate choice for the candidates is isolated tracks within the muon acceptance region. Once the probability is determined, the estimation of the number of events caused by fake muons can be found by looking at all the possible events containing at least one muon and one candidate object, after weighing them by the muon fake probability. This method has been validated for loose selection criteria on the candidates [13]. Once data is available the selection criteria will be refined so that they match our muon selection as closely as possible.

5 Standard Model Background Estimation

The $t\bar{t}$, tW, and WZ Standard Model processes are the largest non-QCD backgrounds to the signature studied in this note. We can estimate these backgrounds by using a control region of two like-sign different-flavor leptons, specifically $e\mu$. The background is obtained by counting the number of events where the decay produces two lepton flavors, e and μ, with the same sign. The kinematics is identical to the like-sign $\mu\mu$ production so that, after correcting for the difference in selection efficiency, reconstruction efficiency and acceptance between the muon and the electron, the number of $e\mu$ events should be twice that of the number of $\mu\mu$ events:

$$N_{\mu\mu}^{est} = \frac{N_{\mu\mu}^{exp}}{N_{e\mu}^{exp}} \times N_{e\mu}^{obs} = \frac{A}{2} \times N_{e\mu}^{obs} \tag{4}$$

$$A = \frac{A_{\mu\mu} \times \epsilon_{SS\mu\mu}}{A_{e\mu} \times \epsilon_{SSe\mu}} \tag{5}$$

where A denotes the ratio of kinematic acceptance ($A_{\mu\mu}$ and $A_{e\mu}$) times the selection efficiencies for $\mu\mu$ ($\epsilon_{SS\mu\mu}$) and $e\mu$ ($\epsilon_{SSe\mu}$) events. To be sure that the method works as expected the samples are divided into two. The ratio is found by looking at the events from the first part of the Monte Carlo data set, while the other part is used to find the $N_{e\mu}^{obs}$. In this ratio many of the uncertainties cancel. However, fake rates and wrong charge assignments for the electrons must be studied with the data. The electron fake rate may be determined with a similar method to that described for understanding the muon fake rate. The appropriate candidates in this

Table 7: The number of events in 100 pb^{-1} for the control and signal regions, as well as the number of events expected from the calculation based upon the control region is shown. The Monte Carlo statistical uncertainty is shown.

process	$N_{e\mu}^{obs}$	A	$N_{\mu\mu}^{est} \pm \Delta N_{\mu\mu}^{est}$	$N_{\mu\mu}^{obs}$
$t\bar{t}$	2.89	1.18	1.71 $\pm$0.33	1.50
WZ	0.95	2.69	1.28 $\pm$0.20	0.23
tW	0.23	0.76	0.086 $\pm$0.027	0.076

case are jets, but the method is otherwise the same [13]. We expect that the uncertainties will become much lower with increased integrated luminosity. Detailed analysis will be performed to obtain systematics once the data becomes available [14], and 20% systematical uncertainties were used as a conservative number in the current analysis [15]. This method will not be practical until the single-lepton efficiencies are well measured from the $Z \rightarrow l^+l^-$ after 100 pb^{-1} the uncertainties that don't cancel should then be small [16]. The Monte Carlo will be tuned to match these measured efficiencies.

We select the control samples by using identical cuts for the jets and the single muon, while also requiring an isolated high quality electron with $p_{\mathrm{T}} > 15$ GeV. The electron isolation and quality cuts are identical to those used in study of measuring the WW production cross section at the LHC during start-up collisions [15] and the same p_{T} cut is used for the electron as is used for the muon. As in the analysis we required exactly two like-sign leptons, so if there is exactly one muon and one electron with the same sign, the event is included in the control sample. The number of events at 100 pb^{-1} are summarized in Table 7.

This method works well for the $t\bar{t}$ and tW Standard Model processes; however it doesn't work for the WZ background. This is because there are two mechanisms for like-sign lepton production to occur while there is only one process which produces different lepton flavors. To produce two leptons with different flavors the W and Z must both decay leptonically; this can also produce two like-sign muons, but this background is suppressed by our jet selection. The dominant process for events which pass the like-sign muon selection cuts and jet selection requirements is sign misidentification of a leptoincally decaying Z boson and two jets from a hadronically decaying W. We expect that if the jet p_{T} selection cuts are relaxed the dominant process would instead be one where both both the W and the Z bosons decay leptonically. This should match the dominant process for creating like-sign different flavor leptons, and it corresponds an expected $N_{\mu\mu}^{MC}$ of 1.66 in 100 pb^{-1}. The number of events in the control region should now be very similar to the number of like-sign muons events after the differences in selection efficiencies for the muon and the electrons from the gauge boson decays are corrected for. The $N_{e\mu}^{obs}$ is 1.23 events in 100 pb^{-1} when the jet selection cuts are relaxed the resulting $N_{\mu\mu}^{exp}$ is 1.65 which which is very close to the value found from the standard analysis.

6 Discovery Significance and Errors

There are two main sources of systematic uncertainties in our study; the theoretical uncertainties in the matrix element calculations, and the detector effects, primarily from the jet reconstruction. The theoretical uncertainties in the Majorana neutrino production have been examined in detail [2]. The QCD correction and other QCD uncertainties due to our choice of Q^2 scale are combined to give us a 20% theoretical uncertainty. The background estimation will also be affected by uncertainties in the cross sections of the different processes. The actual

Table 8: Summary of the uncertainties in background estimation and the resulting change in the background yield. As well as the expected number of background events.

Error	Input	N_B at 100 pb^{-1}	$\pm\Delta N_B$ at 100 pb^{-1}
$t\bar{t}$ σ	$\pm$50%	1.5	0.75
$WW/ZZ/WZ$ σ	$\pm$20%	< 0.34	< 0.068
tW σ	$\pm$20%	0.076	0.015
DY/$Z\rightarrow$ $\mu\mu$ σ	$\pm$20%	0.14	0.028
$Z\rightarrow$ $\tau\tau$ σ	$\pm$20%	< 0.086	< 0.017
VQQ σ	$\pm$20%	0.029	0.0058
QCD	$\pm$100%	2.9	2.9
Jet Energy Scale	$\pm$10% per jet		0.24
b-tagging	$\pm$8.5%		0.23
MC Statistics			0.66
Total		5.01	3.1

systematical uncertainties will be measured from data when they becomes available. In this analysis, we assume conservative uncertainties in the cross section values for the backgrounds gauge boson backgrounds of 20% [15, 17]. Based upon the results from our different flavor like-sign lepton study we assign an uncertainty on the largest non-QCD background, $t\bar{t}$, of 50%.

Currently the jet energy scale corrections are all based upon Monte Carlo estimations. Since the systematics uncertainties in jet energy scale will likely be dominated by effects in the real collider that cannot be anticipated there has not yet been any official estimations of the systematic uncertainties in jet energy. It is expected that the initial systematic uncertainties can be kept to about 10% using the simulation results [10]. Based on these assumptions, we have processed our Monte Carlo data while smearing the jet energy by $\pm$10%, and calculated an error to the discovery significance based upon the resulting new mass reconstruction histograms. The systematic uncertainty in the b-tagging is expected to be about 8.5% for 100 pb^{-1} [18]. We adjusted the b-tagging rates by this amount in the analysis. The charge misidentification rates for muons with p_{T} near 100 GeV, the upper range of p_{T} region we study, is expect to be below 0.001 for the global and tracker fits; further is expect to be below 1.0×10^{-5} for the tracker fits of muons with p_{T} near 10 GeV [8]. We analyzed the background applying a muon charge mis-id rate ten times the expected values, and this did not have a significant affect on the expected number of background events. The other systematics dominate the uncertainties. A summary of the systematic uncertainties uses is show in Table 8.

The early data from the LHC should give us the ability to increase the lower limits on the mass of a potential Majorana neutrino. We have investigated the possibility of discovery or exclusion through excess events with the early LHC data. For a M_N near 100 GeV the theoretical cross section is large enough that the expected total number of signal events is significantly larger than the total amount of background. However, in the upper limit the number of background events and the number of expected signal events is nearly equal. This is due largely to the QCD background which is dominated by the $\hat{p}_T$ range between 30 and 80 GeV. The reconstructed mass from the QCD background is dominated by the selection of two jets near the W mass peak well below the upper limit of the mass range studied. To take advantage of this our calculations look for excess within binned mass ranges (Table 9). Near 100 GeV we can use a narrow bin of $\pm 1.5\sigma$ (90-130 GeV) as the mass peak is very clear (Fig. 6), as the M_N increases we widen

Table 9: The binned mass ranges used for the calculation of discovery or exclusion limits through excess events.

	Bin Limits (GeV)		Num. Events (100 pb^{-1})		
M_N (GeV)	Lower	Upper	QCD BG	Total BG	Signal
100	90	130	1.03	1.91	38.3
120	100	150	1.09	1.93	27.3
140	110	170	1.11	1.93	16.8
160	120	190	1.06	1.82	10.8
180	130	210	0.828	1.59	7.03
200	140	230	0.676	1.16	4.79

the bin on the lower side to allow for the incorrect choice of muon using a bin of 140-230 GeV for calculations with respect to the 200 GeV Majorana neutrino mass . As no QCD event is are accepted by the selection criteria we estimate the number of QCD events within each binned mass region from the distribution of reconstructed masses from QCD events with 2 jets with p_{T} above 30 GeV and one global muon with p_{T} above 15 GeV. The probability for the number of expected background events to fluctuate to or above the expected number of observed events if there is new physics was calculated for each mass bin. The background was allowed to fluctuate with the uncertainty of 61.9%. Discovery over about half of the mass range studied should be possible with 100 pb^{-1} integrated luminosity (Fig 6). We don't assume the potential for discovery below 100 pb^{-1} because the systematical uncertainties in the backgrounds will not be well understood before that point.

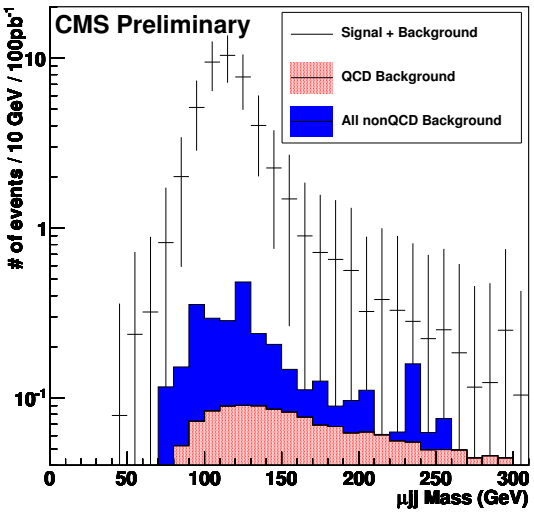

Figure 6: The μjj invariant mass of the M_N and the backgrounds. The 100 GeV M_N data set is shown with 100 pb^{-1} integrated luminosity. We can use this mass distribution to understand how we might set the limits on the binned mass range used for our calculations of potential discovery due to excess events.

If no excess is found, exclusion of the entire mass range studied should be possible with 100 pb^{-1} of data. We obtained 95% Bayesian confidence limits to set our exclusion.The calculation was done following the same procedure as described in [19], where a standard Bayesian approach [20] is utilized with a flat prior chosen for the signal cross section. The Poisson likelihood of observing a given number of events in data given our cross section, signal acceptance, background cross sections and integrated luminosity is calculated. This is convoluted with

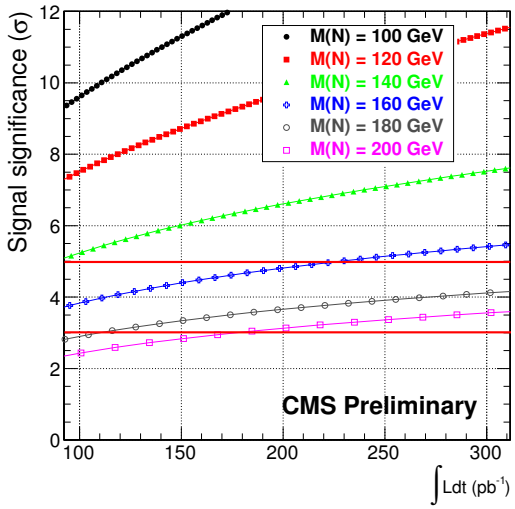

Figure 7: The discovery significance vs the integrated luminosity for several masses within the region studied. The 3σ and 5σ lines are shown in red.The significance values below 100 pb^{-1} do not include the increased uncertainties in the measurements; therefore, we don't assume the significance values for that region to be valid for discovery.

Gaussian distributions around each parameter to account for the systematic uncertainties. The 95% upper limit is found by solving the integral equation with all the the uncertainties integrated out.

7 Conclusion

The CMS detector should be able to discover a Majorana neutrino with a mass less than 200 GeV in the early data if excess events are seen. If no excess events are seen the Majorana neutrino mass range up to 200 GeV can potentially be excluded. A method for controlling the largest background of $t\bar{t}$ has been outlined, and an estimation of the QCD background has been discussed.

8 Acknowledgments

We thank Steve Mrenna for his help during the simulation of the signal, Francisco Yumiceva for his assistance with our working with the *b*-tagging algorithms, and Greg Landsberg and Albert De Roeck for their advice and guidance in performing this analysis.

References

[1] For earlier comprehensive discussions of neutrino physics see *e.g., Massive Neutrinos in Physics and Astrophysics* by R. N. Mohapatra and P. B. Pal (World Scientific 2004); *Physics of Neutrinos and Applications to Astrophysics* by M. Fukugita and T. Yanagida (Springer-Verlag 2003). For recent reviews, see *e.g.,* V. Barger, D. Marfatia, and K. Whisnant, Int. J. Mod. Phys. **E12**, 569 (2003); B. Kayser, p. 145 in PDG in Phys. Lett. **B592**, 1 (2004); M.C. Gonzalez-Garcia and M. Maltoni, arXiv:0704.1800 [hep-ph]; R. N. Mohapatra and A. Y. Smirnov, Ann. Rev. Nucl. Part. Sci. **56** (2006) 569; A. Strumia and F. Vissani, arXiv:hep-ph/0606054.

[2] A. Atre, T. Han, S. Pascoli and B. Zhang, "The Search for Heavy Majorana Neutrinos," arXiv:0901.3589 [hep-ph].

[3] M. R. Wahlley, D. Bourilkov, and R. C. Group, "The Les Houches Accord pdfs (lhapdf) and lhaglue," (2005) arXiv:hep-ph/0508110v1

[4] T. Sjostrand, S. Mrenna, P. Skands, "PYTHIA 6.4 Physics and Manual," JHEP 05 (2006)026

[5] Agostinelli S, et al. GEANT4-a simulation toolkit NIM A 506 (3): 250-303 Jul1 2003

[6] A.S. Belyaev et al, "CompHEP - PYTHIA interface: integrated package for the collision events generation based on exact matrix elements, in: Advanced computing and analysis techniques in physics research" (Proc. of ACAT'2000, Fermilab, 16-20 October 2000), p.211 (arXiv:hep-ph/0101232)

[7] The CMS Collaboration, "CMS High Level Trigger," CERN/LHCC 2007-021, 29 June 2007

[8] CMS Collaboration, CMS Technical Design Report Volume I: Detector Performance and Software, CERN/LHCC 2006-001, 2006

[9] CMS Collaboration, Physics Technical design Report Volume I: Physics Performance, CERN/LHCC 2006-026, 2006

[10] The CMS Collaboration "The CMS plans for providing jet energy corrections in a factorized approach are described" CMS PAS JME-07-002

[11] The CMS Collaboration "Algorithms for b Jet Identification in CMS" CMS PAS BTV-09-001

[12] The CMS Collaboration "Search for Heavy Bottom-like Forth Generation Quark Pair Production at CMS in pp Collisions at $\sqrt{s} = 14$ TeV," CMS PAS EXO-08-009

[13] The CMS Collaboration "Search for the Higgs boson in the WW decay channel" CMS PAS HIG-08-006

[14] The CMS Collaboration "Measuring Electron Efficiencies at CMS with Early Data" CMS PAS EGM-07-001

[15] The CMS Collaboration "Prospects for measuring the WW production cross section in pp collisions at 10 TeV C.O.M." CMS PAS EWK-09-002

[16] N.Adam et al., Towards a Measurement of the Inclusive $W \to e$ and $Z \to ee$ Cross Section in pp Collisions at $\sqrt{s} = 14$ TeV, CMS PAS EWK-07-001. G.Daskalakis et al., Measuring Electron Efciencies at CMS with Early Data, CMS PAS EGM-07-001.

[17] The CMS Collaboration "Search for b' into tW at 10 TeV" CMS PAS EXO-09-012

[18] The CMS Collaboration "b tag Efficiency from System 8 and Ptrel Method" CMS PAS BTV-07-001

[19] The CMS Collaboration "Search for Large Extra Dimensions in the Diphoton Final State" CMS PAS EXO-09-004

[20] I. Bertram et al. FermilabTM2104 (2000).